ISSN 1392-1207. MECHANIKA. 2019 Volume 25(6): 434–441

Experimental Investigation of Water Droplet Heating in Humidified Air Flow

Virginijus RAMANAUSKAS*, Egidijus PUIDA, Gintautas MILIAUSKAS***, Linas PAUKŠTAITIS******

**JSC "Enerstena", Ateities pl. 30 a, LT-52317 Kaunas, Lithuania, E-mail: Virginijus.Ramanauskas@enerstena.lt*
***Kaunas University of Technology, Studentų 56, Kaunas, LT-51424, Lithuania, E-mail: egidijus.puida@ktu.lt*
****Kaunas University of Technology, Studentų 56, Kaunas, LT-51424, Lithuania, E-mail: gintautas.miliauskas@ktu.lt*
****Kaunas University of Technology, Studentų 56, Kaunas, LT-51424, Lithuania, E-mail: linas.paukstaitis@ktu.lt*

crossref http://dx.doi.org/10.5755/j01.mech.25.6.23795

Nomenclature

a - thermal diffusivity, m^2/s; A is area, m^2; D - mass diffusivity, m^2/s; G - mass flow rate, kg/s; $\bar{g}_v$ - water vapour mass fraction in gas; l_k - width of the experimental test section, m; M - mass, kg; M_μ - molecular mass, kg/kmol; p - pressure, Pa; $\bar{p}_v$ - water vapour volume (molar) fraction in gas mixture; T - temperature, K; t - temperature,°C; R - radius of a droplet, m; R_μ - universal gas constant, J/(kmol·K); ρ is density, kg/m^3; τ - time, s; w - velocity, m/s; φ - relative humidity, %.

Subscripts: B - barometric; co - condensation; dp - dew point; dr - dry; e - equilibrium evaporation; f - phase change; g - gas mixture (additionally humidified air); l - water; m - mass average; o - ambient air; tb - thermocouple bead; R - droplet surface; s - saturated; v - vapour; 0 - droplet initial state.

1. Introduction

Fossil fuel resources are still sufficient to meet the modern energy needs of mankind [1]. However, natural gas and oil resources have a wide range of industrial applications and should be used responsibly in traditional energy production technologies. In addition, the burning of fossil fuels has a negative impact on the environment of the modern world [2]. So it is relevant to reduce the fossil fuel component in the overall energy balance [3]. In this aspect, it is efficient to develop renewable energy source (RES) technologies [4]. Resources from RES, their sustainability and the prospect of exploitation are assessed and based on scientific analysis [5-7]. Biomass and biofuels occupy the predominant position in RES [6], that is why biofuel and its combustion technologies are being introduced into domestic use [8], transportation [9], electricity and thermal energy production [10-12].

Modern biofuel technologies are widely used [13-18]. The applicability of liquid spraying, for improvement the efficiency of the biofuel combustion process and enhancing environmental impact, is prominent. Therefore, in the global energy industry, the development of biofuel technologies defines the growing interest for droplets evaporation process and its influence for fuel burning characteristics [19-22]. Water droplet and sprays are also suitable for combustion control [18, 23] and reduction of toxogens concentrations in combustion products [18, 24, 25], for cooling of flue gas [26] and recovery of heat [27, 28]. The efficiency of liquid spray technology is determined by the intensity of the droplet transfer processes and the very high contact surface between the liquid and gaseous phases. Therefore, the research of the sprayed liquid droplets heat and mass transfer is popular and its history has been over a century [29]. However, interest is not decreasing in this subject [30]. This is owing to the need of improvement of existing and development of new spraying technologies. This requires a good understanding of the heat and mass transfer processes of the sprayed liquid droplets, and droplet studies are conducted in various aspects [26, 29-36]. The boundary conditions of the water droplets phase change and heat transfer in biofuel combustion technologies can be very different. Two very important cases of water spraying can be distinguished.

In the first case, the water is sprayed to regulate the combustion process in the furnace. Water can also be sprayed to the flue gas, flowing from the furnace. The purpose of this action is to suppress the nitrogen oxides formation and reduce atmospheric pollution. When the water is sprayed into biofuel furnace flue gas, the droplets must completely evaporate. This allows to use the traditional ferrous-metal-based heat exchangers for cooling flue gas and does not create favorable conditions for wall corrosion. In the second case, water is sprayed into technologically cooled flue gas with the purpose to improve the heat recovery process before releasing flue gas into the atmosphere. Heat from removed flue gas is recovered in condense economisers. The biofuel flue gas average temperature is 130-180°C and average water vapour volume fraction is 0.2-0.35 in gas mixture. The flue gas is cooled to temperature of 40°C and during condensation process water vapour volume fraction decreases to 0.07 in average. In this case, the efficiency of the condense economiser is defined by the drying of the flue gas, because in the water vapour condensation process the released heat is significantly higher than the heat, which is recovered from the cooled flue gas. It is important to cool the flue gas down to the dew point temperature before the heat exchanger. For this, the primary water injection is performed. Inside flue gas economizers water is sprayed in order to condense the vapour on the droplets (for a case of contact heat exchanger) or to improve the hydrodynamics of the condensate and polluted flue gas (for a case of recuperative heat exchanger). In modern biofuel combustion technologies, the flue gas is well cleaned of pollutants.

A literature review indicates that the droplet heat and mass transfer processes are important for liquid spraying technologies, which were investigated when applying the theoretical and numerical modelling and experimental

methods. Modern numerical heat and mass transfer of droplets models allow to define complex transient transfer processes. These models take into account the Stefan's hydrodynamic flow, the specificity of spectral radiation absorption in a semi-transparent liquid, the influence of transit regimes, and other factors that determines the interaction of the complex transfer processes. The main factors which define the phase change of the water droplets in the biofuel flue gas are the temperature, the humidity of a gas flow and the sprayed water temperature [34]. An important factor is the boundary conditions of the droplets heat transfer, that are influenced both by the slipping of a droplets in the gas and by the emissivity of the droplets surrounding.

The application of a numerical modelling is perspective, but experimental research results that required for control are insufficient, particularly in cases of transient phase changes of water droplets in humid flue gas flow. However, it should be noted that the experimental investigations are needed to control numerical models results is still insufficient in transient regimes of complex transfer processes, especially in water vapour condensation regime on a droplet surface. The water vapour condensation and water transient evaporation regimes are particularly important for defining the optimal water spraying in biofuel combustion technologies

In this work results of experimental research on the heating of water droplets in purified biofuel flue gas were presented and analyzed. In experimental investigation the purified biofuel flue gas is replaced by additionally humidified air flow. The experiment methods and results processing are discussed and provided. Impact of air heating and additional humidification was estimated. While heating and additionally humidifying the air flow was focused on boundary conditions in condense economisers, when the flue gas temperature is 20 ÷ 100°C and water vapour volume fraction is 0 ÷ 0.2.

2. Experiment method and processing of the results

The principal scheme of the experimental setup is presented in Fig. 1. The main components are: air flow heater *4*, the water evaporator *5* for additional humidification of the air flow, the experimental test section *7* and the special system *10* for the water droplet introducing into the experimental section. Other components of the experimental setup are designed for the data collection and processing. The temperature, humidity, and pressure of environment air are measured using a TESTO 445 device *1*. The air blower *2* supplies the air to the heater *4*, where the air flow is heated to the set temperature. The air speed and temperature is measured with anemometer *3* after the blower in a pipe of 80 mm diameter and 1 m length. The water vapour from evaporator *5* is supplied in the air flow and the amount of evaporated water is measured using scales *6*. The heated and additionally humidified air flow is supplied into the experimental test section *7*.

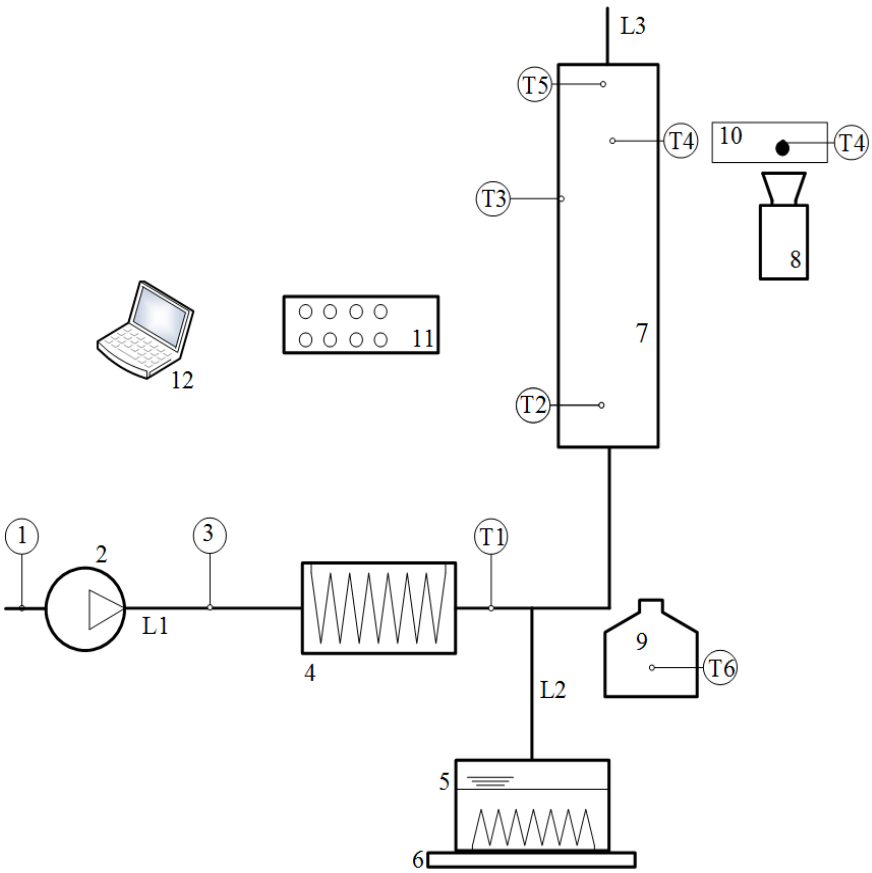

Fig. 1 Principal scheme of the experimental set-up. *1* – air temperature, humidity and pressure meter; *2* – centrifugal blower; *3* – air speed and temperature meter; *4* – air heater; *5* – water evaporator; *6* – scales; *7* – experimental test section; *8* – photo camera; *9* – water tank for droplet formation; *10* – system for water droplet introduction into the experimental section; *11* – temperature measurement and data storage; *12* – computer used for data acquisition and processing; T1, T2, T3, T4, T5 and T6 – thermocouples; L1 – pipe for air inlet; L2 – connecting pipe between the main airline and evaporator; L3 – air flow discharge pipe

After passing the test section *7* the humid air flows out from the experimental setup in pipe L3. Thermocouples T2, T3 and T5 are used to measure the temperature of the humid air flow at different segments of *7*. Water droplet is formed by the pipette on a thermocouple T4 and is introduced by a special system *10* into the experimental section *7*. The water for the droplet is taken from the container *9*. The water temperature is measured by the T6 thermocouple. All thermocouples are connected to the Pico Logger TC-08 data logger, while the logger is connected to a computer *12*.

An initial droplet size is taken by photo camera *8*. Data obtained from a video camera is analyzed using an image recognition program according to the methodology of work [37] and written in MATLAB. The initial equivalent diameter of the droplet is defined with an average confidence of ± 0.04 mm. The equivalent diameter of the droplet $2R$ is perceived as a diameter of sphere of combined volume of the thermocouple bead and the water which surrounds it.

The accuracy of experiment is determined by measuring devices and their descriptions provided and certified by the manufacturers. A Pico-Logger TC-08 has a temperature measurement accuracy of ±0.38°C. The equivalent diameter of the thermocouple bead is measured using a micrometer with accuracy of ± 0.02 mm. The TESTO 445 measures air temperature, relative humidity and pressure at accuracies of ± 0.3°C, ± 2% rH and ± 0.01 hPa for respectively. In the evaporator, the evaporated water mass was measured with an accuracy of ± 0.5 g.

The experiments are performed consistently in the steps described below: The ambient air relative humidity φ, %; temperature t_o,°C and barometric pressure p_B, Pa are measured; Velocity w_o, m/s; of the air flow is measured in the 80 mm diameter tube L1 (the air flow velocity is set by adjusting the performance of the centrifugal blower); For an additional air flow humidification, the amount of water vapour, which is supplied to the experimental section, is controlled by the electric load of the evaporator; A droplet is formed on the thermocouple bead with an indicative temperature t_l,°C, and the thermocouple logger starts to record its temperature; A special insertion system with a safety glass tube positions the water droplet into the centre of the experimental section; At the moment when the safety glass tube is removed, the condition $\tau_1 = 0$ is assumed and the initial droplet temperature t_0,°C and water mass M_1, kg in evaporator are fixed; The experiment is continued until the droplet water completely evaporates and the thermocouple bead warms to the gas flow temperature t_g,°C. Then the time τ_2, s and water mass M_2, kg in evaporator are fixed.

The results of each experiment are processed consistently in the following order:

1. The water vapour partial pressure in ambient air is determined as $p_{v,o} \equiv p_s(t_o)$, Pa. Then the volumetric $\overline{p}_{v,o}$ and mass $\overline{g}_{v,o}$ fractions of water vapour in the ambient air are defined as follows:

$$\overline{p}_{v,o} = \frac{\varphi}{100}\frac{p_{v,s}(t_o)}{p_B}, \tag{1}$$

$$\overline{g}_{v,o} = \frac{\overline{p}_{v,o} M_{\mu,v}}{\overline{p}_{v,o} M_{\mu,v} + (1-\overline{p}_{v,o}) M_{\mu,o,dr}}. \tag{2}$$

2. The air flow rate G_o, kg/s is calculated and the vapor flow component $G_{v,o}$, kg/s is defined as follows:

$$G_o = A_{L1}\rho_o w_o, \tag{3}$$

$$G_{v,o} = \overline{g}_{v,o} G_o. \tag{4}$$

3. The additionally humidified air flow rate G_g, kg/s and the vapor flow component G_v, kg/s is calculated as follows:

$$G_v = G_{v,o} + \frac{M_2 - M_1}{\tau_2 - \tau_1}, \tag{5}$$

$$G_g = (1-\overline{g}_{v,o})\cdot G_o + G_v. \tag{6}$$

4. The mass $\overline{g}_{v,g}$ and volumetric $\overline{p}_{v,g}$ fractions of water vapour in the gas are defined as follows:

$$\overline{g}_{v,g} = \frac{G_v}{G_g}, \tag{7}$$

$$\overline{p}_{v,g} = \frac{R_\mu / M_{\mu,v}}{R_\mu / M_{\mu,v} - (1 + 1/\overline{g}_{v,g})(R_\mu / M_{\mu,o,dr})}. \tag{8}$$

5. The partial pressure p_{vg}, Pa of the water vapour in the gas is calculated and the dew point temperature t_{dp},°C is defined as follows:

$$p_{v,g} = \overline{p}_{v,g} \cdot p_B, \tag{9}$$

$$t_{dp} = t_s(p_{v,g}). \tag{10}$$

6. The velocity of gas w_g, m/s flow in the experimental setup is calculated:

$$w_g = \frac{G_g}{\rho_g l_k^2}; \quad l_k = 0.05 \text{ m}. \tag{11}$$

7. The hydrodynamics regimes of gas flow and droplet overflow are determined by Reynolds numbers respectively:

$$Re_g = \frac{w_g l_k}{\nu_g}; \; Re_l = \frac{2 w_g R}{\nu_g}. \tag{12}$$

8. According to droplet temperature measuring results the droplets heating thermogram $t_l(\tau)$ is composed.

3. Experimental results and discussion

The experiment was performed for the regularities definition of water droplet thermal state variation in humid air flow as well for verification of theoretical conclusions presented in work [34]. The experiment focused on the water injection cases in flue gas condensers. For the definition of optimal water spraying it is necessary to select properly

the sprayed water temperature in order to ensure the suitable droplet transient evaporation regimes, because it is important to achieve the desired technological goal as effectively as possible. The experiments were conducted with large water droplets, which equivalent diameter were 2-3 mm. The hydrodynamics regimes of gas flow and droplet overflow are determined by Reynolds numbers $Re_g = 10000 \div 20000$ and $Re_l = 400 \div 1000$ respectively. Experiment was performed in two stages.

In the first stage, the influence of additionally humidified air for the droplet heating is investigated (Figs. 2 and 3). In the second stage of the experimental research, the impact of the initial water temperature on the thermal state change of a droplet was studied in more detail (Figs. 4 and 5). It is important to know this influence when defining the optimal regimes of sprayed water in different biofuel combustion technology devices. The transfer processes of a droplet are analyzed in the cycle of phase change regimes on a droplet surface. The beginning of the phase change cycle is defined by moment $\tau = 0$, while the end is fixed by a water evaporation moment $\tau = \tau_f$. In the cycle take place the transit phase transformation $\tau \equiv 0 \div \tau_e$ and the equilibrium evaporation $\tau \equiv \tau_e \div \tau_f$ regimes. In the transit phase transformation regime such processes as liquid vapour condensation on a droplet and liquid evaporation from a droplet surface can take place [34].

The initial temperature $t_0 = t_l(\tau = 0)$ of the water droplet, placed on the thermocouple bed, was fixed according to temperature of its introduction moment into the air flow. The droplet temperature variations $t_l(\tau)$ thermogram is created according to the droplet temperature measurement every second results (Fig. 2 and 4). After water evaporates, the temperature of the air flow t_g is determined based on the temperature of the thermocouple bead (Fig. 3 and 5).

In the first stage of the experimental research the condition $t_0 < t_e$ was valid, the supplied air flow rate is $9.244 \cdot 10^{-3}$ kg/s, the temperature is 19.4°C, the relative humidity is 56.8% and the pressure is 989 hPa.

In the first experiment this air flow was heated to temperature above 96°C, and overflowed droplet with an initial temperature of 31.7°C in the experimental section. The droplet temperature during transient evaporation regime increased by 10.8°C and reached $t_{e,1} = 42.5$°C temperature (Fig. 2, curve *1*). During equilibrium evaporation regime the droplet warms an additional of 3.3°C and reached $t_{f,1}$=45.8°C temperature (Fig. 3, curve *1*). After water fully evaporates, the thermocouple bead rise to 96.6°C temperature (Fig. 3, curve *1*).

In a second experiment, the air flow was additionally humidified with a vapour flow of $0.194 \cdot 10^{-3}$ kg/s from the water evaporator. The volumetric fraction of water vapour in the gas flow was increased from 0.0129 to 0.045. This additionally humidified gas flow into the experimental section and overflows a droplet with an initial temperature of 30.3°C.

In the second experiment, the droplet temperature during transient evaporation regime increased by 24.6°C and reached $t_{e,2}$=54.9°C temperature (Fig. 2, curve *2*). During equilibrium evaporation regime the droplet warms an additional of 1.9°C and reached $t_{f,2}$=56.8°C temperature (Fig. 3, curve *2*). After water fully evaporates, the thermocouple bead rise to 96.5°C temperature (Fig. 3, curve *2*).

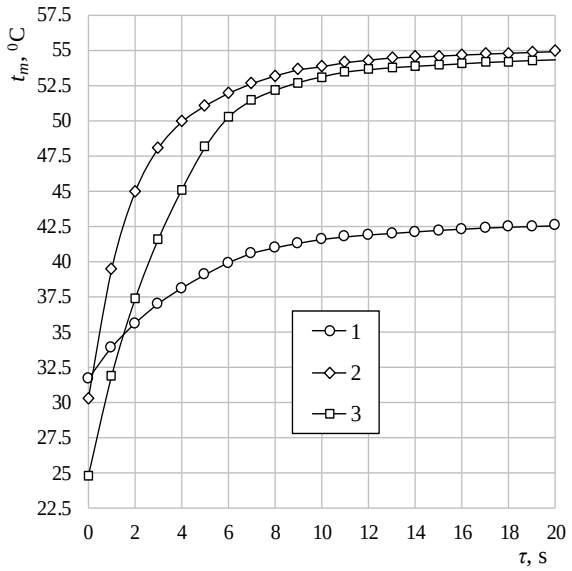

Fig. 2 Heating process of the water droplet in heated ambient air flow *1* and in additionally humidified gas flow *2*, *3* in the transient phase change regime. t_o=19.4°C; φ_o=56.8%; p_B=989 hPa; G_o=$9.244 \cdot 10^{-3}$,°kg/s; $G_v \cdot 10^3$, kg/s: *1* 0, *2*, *3* 0.194; t_g,°C: *1* 96.6, *2* 96.5, *3* 96.1; w_g, m/s: *1* 3.99, *2*, *3* 4.12; $\overline{p}_{v,g}$: *1* 0.0129, *2*, *3* 0.045; t_{dp},°C: *1* 10.62, *2*, *3* 30.84; t_0,°C: *1* 31.7, *2* 30.3, *3* 24.7

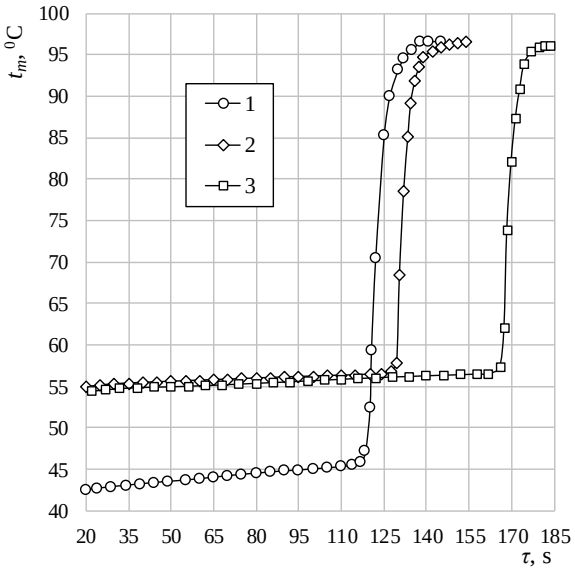

Fig. 3 The variation of the droplet temperature in equilibrium evaporation regime and the thermocouple bead heating to the flow temperature in heated ambient air flow *1* and in additionally humidified gas flow *2*, *3* in the equilibrium evaporation regime. The experimental boundary conditions are as shown in Fig. 2

It must be said that in both cases, the gas temperature is practically the same, and the gas flow rate in the test section channel is similar. Therefore, the droplet higher $t_{e,2}$-$t_{e,1}$=12.4°C heating in the additionally humidified gas flow in the transient phase transition regime can only be explained by the significant effect of the humidifying air on the droplet equilibrium evaporation temperature. In this case, the volumetric fraction of water vapour in the additionally humidified gas was increased almost 3.5 times. The slight droplet heating in the equilibrium evaporation regime

can be explained by additional droplet heating through the thermocouple wires. Its influence for the heat transfer of the droplet water and thermocouple bead system increases, when the mass of the droplet consistently decreases in the process of the water equilibrium evaporation.

In a third experiment, the droplet heating was repeated, and the results of the second experiment were practically confirmed when a flow of additionally humidified and heated air was used. The water droplet of slightly lower initial temperature of 24.7°C in the transient evaporation regime heats by 29.5°C and reached $t_{e,3}$=54.2°C temperature (Fig. 2, curve *3*), and in equilibrium evaporation regime heats by 2.4°C and reached $t_{f,3}$=56.6°C temperature (Fig. 3, curve *3*). The droplet temperature $t_{f,3}$ was 0.2°C lower due to a slightly lower air flow temperature of 96.1°C at the end of the equilibrium evaporation regime. In the beginning of the equilibrium evaporation regime, the 0.7°C lower droplet temperature $t_{e,3}$ is influenced by the uneven boundary conditions of droplet heat transfer in the time moment τ_e.

For ambient air flow the dew point temperature is 10.62°C, and for additionally humidified gas flow the dew point temperature is 30.84°C. The dew point temperature t_{dp} is defined based on the Gerry correlation [38]. For heated ambient air flow, the experiment was carried out in condition $\bar{t}_{dp} \equiv t_{dp} / t_0 = 0.355$. In the case of additionally humidified gas flow, conditions of $\bar{t}_{dp} = 1.018$ and $\bar{t}_{dp} = 1.249$ were valid for the second and third experiments, respectively. Therefore, the required condition $\bar{t}_{dp} > 1$ for the condensation phase change regime on the droplet surface was fulfilled in the second and third experiments cases. In this cases during condensation phase change regime the droplet surface temperature reaches the dew point temperature. Because the relative slipping of a droplet in air flow is high, therefore the intensive forced circulation of water caused by the friction forces will take place inside the droplet [39]. Therefore, the droplet surface temperature is close to the water mass mean temperature, and duration of a condensation regime is defined by condition: $\approx \tau_{co} = \tau\left[T_m(\tau) \equiv T_{dp}\right]$. The duration of the condensation regime $\approx \tau_{co}$ is 0 s, 0.16 s, and 0.92 s for first, second and third experiments, respectively. The calculated duration of the transient phase change regime of a sprayed water droplet is clearly defined by the time moment when the droplet heats up to the highest temperature $\tau_e = \tau\left(t_l \equiv t_{l,\max}\right)$ [34]. In the experiments the droplet temperature increases in equilibrium evaporation regime (Fig. 3). Therefore, it is only possible to define the duration of the transient phase change regime indicatively: in the first experiments $\tau_e \approx 18$ s , in the second and third experiments $\tau_e \approx 20$ s. The duration τ_f of the droplet phase change is defined by the water evaporation moment $\approx \tau_f = \tau\left(2R \equiv 2R_{tb}\right)$. In the first, second, and third experiments, $\approx \tau_f$ is 117.7 s, 128.1 s, and 165.5 s, respectively.

At the second stage of the experimental research, eight experiments were conducted. The experiment focused on the water injection cases in flue gas condensers for heat recovered of the removed biofuel flue gas. For the definition of optimal water spraying it is necessary to select properly the sprayed water temperature in order to ensure the suitable droplet transient evaporation regimes, because it is important to achieve the desired technological goal as effectively as possible. Therefore, in all experiments, the initial temperature of the water droplet was different. In 3, 5, 6 and 7 experiments the condition $t_0 < t_e$ was valid, and in 1, 2, 4 and 8 experiments the condition $t_0 > t_e$ was valid (Fig. 4). In the experiments (1-4) the volumetric fraction of the water vapour in the ambient air is approximately 0.0087 and the dew point temperature is 4.97°C.

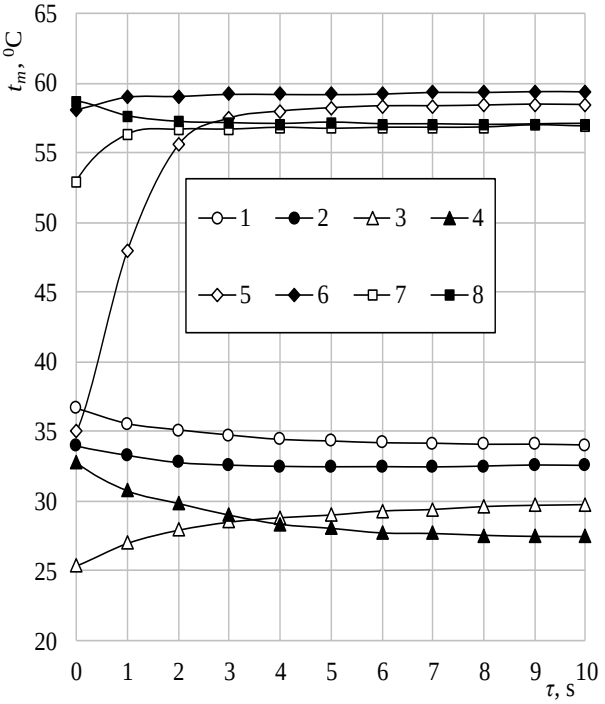

Fig. 4 Influence of the water initial temperature to heating process of the droplet in heated ambient air flow *1-4* and in additionally humidified gas flow *5-8* in the transient phase change regime. t_o=21°C; φ_o=35%; p_B=1000.3 hPa; G_o=15.88·10^{-3}, kg/s; G_v·10^3, kg/s: *1-4* 0, *5-8* 1.572; t_g,°C: *1*, *2* 85.6, *3* 62.4. *4* 62.2, *5* 80.9, *6* 81.3, *7* 65.4, *8* 65.5; w_g, m/s: *1*, *2* 6.56, *3* 6.14, *4* 6.13, *5* 7.5, *6* 7.51, *7* 7.18, *8* 7.17; t_0,°C: *1* 36.6, *2* 33.9, *3* 25.4, *4* 32.2, *5* 35, *6* 58.1, *7* 53, *8* 58.7; $\bar{p}_{v,g}$: *1-4* 0.0087, *5-8* 0.1444; t_{dp},°C: *1-4* 4.97, *5-8* 53.23

In the experiments *5-8* the volumetric fraction of the water vapour in the additionally humidified gas is approximately 0.144 and the dew point temperature is 53.23°C. At the same humidity, the droplet heating was mainly determined by the gas temperature and was only slightly influenced by the boundary conditions of convective heat transfer on a droplet (Fig. 4). For the cases *1-4* of heated air, the initial water droplet temperature was changed from 25°C to 37°C. In the transient phase change regime, the droplet heats in case *3* only, while in experiment *1*, *2*, and *4* the cooling of a droplet was noticed (Fig. 4, curves *1–4*)

When the ambient air flow is heated up to ≈ 85,6°C (Fig. 5 a, *1* and *2* curves), the droplet temperature decreased to ≈ 34°C in the transient phase change regime in case *1* (Fig. 4, *1* curve) and in case *2* droplet cools down to ≈ 33°C (Fig. 4, *2* curve). When the ambient air flow is heated up to ≈ 62,2°C (Fig. 5 a, *3* and *4* curves), the droplet temperature increases to ≈ 30°C in case 3 (Fig. 4, *3* curve), whereas in

case *4* droplet cools down to ≈ 27°C (Fig. 4, *4* curve) in the transient phase change regime. For the cases *5-8* of heated and additionally humidified air, the initial water droplet temperature was changed from 35°C to 59°C. In the transient phase change regime, the droplet warms in cases *5*, *6* and *7* (Fig. 4, curves *5–7*), and cools in case *8* only (Fig. 4, curve *8*). When the additionally humidified gas flow is heated up to ≈ 81°C (Fig. 5 b, *5* and *6* curves), the droplet in the transient phase change regime warms up to ≈ 58°C in case *5* (Fig. 4, curve *5*), and warms up to ≈ 59°C in case *6* (Fig. 4, curve *6*). When the additionally humidified gas flow is heated up to ≈ 65.45°C (Fig. 5 b, *7* and *8* curves), the droplet in the transient phase change regime warms up to ≈ 57°C in case *7* (Fig. 4, curve *7*), and in case *8* cool down to ≈ 57°C (Fig. 4, curve *8*).

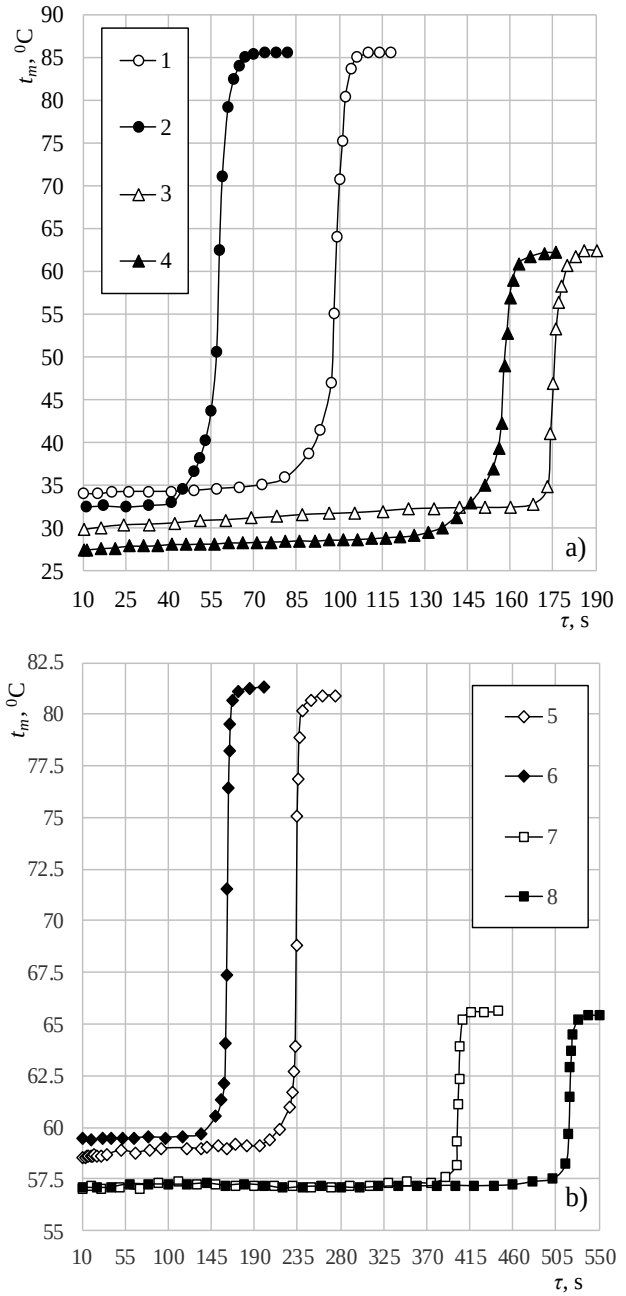

Fig. 5 The variation of the droplet temperature in equilibrium evaporation regime and the thermocouple bead heating to the flow temperature in heated ambient air flow (a) and in additionally humidified gas flow (b). The experimental boundary conditions are as shown in Fig. 4

Therefore, the initial temperature of water significantly influences the change of the thermal state of a droplet both for the only heated ambient air flow and the additionally humidified gas flow cases, depending on the value of the parameter $\bar{t}_e$, what was theoretically defined in [34] work. For cases *3* and *5–7*, the water temperature was lower than the equilibrium evaporation temperature of a droplet and the parameter $\bar{t}_e > 1$ was maintained. Then the droplet warms to the equilibrium evaporation temperature was experimentally confirmed. For cases *1*, *2*, *4*, and *8*, the water temperature was higher than the droplet equilibrium evaporation temperature and the parameter $\bar{t}_e < 1$ was maintained. Then the droplet cooling down the equilibrium evaporation temperature was experimentally confirmed.

4. Conclusions

The results of the experimental investigation of the water droplets heating in the additionally humidified gas flow confirmed the following:

1. In the gas flow the factors determining the phase change regimes of a water droplets are the humidity of the air and the initial temperature of the water. The initial temperature of the water defines the peculiarities of the transient phase change regime of the droplets. The air flow parameters define the droplets equilibrium evaporation temperature, which is not affected by the initial water temperature.
2. The results of the experimental investigation suggest that the dimensionless $\bar{t}_{dp} = t_{dp} / t_0$ and $\bar{t}_e = t_e / t_0$ parameters are appropriate for determining the peculiarities of the water droplets phase change regimes in the humid gas flow. In the disperse water and humidity gas two phase flow the condition $\bar{t}_{dp} > 1$ is necessary to ensure all of the droplets phase changes that consist of condensation, transient evaporation and equilibrium evaporation regimes, and that they proceed sequentially. It has been experimentally confirmed that the water droplets in the initial evaporation stage have cooled, when the condition $\bar{t}_e < 1$ is valid.
3. In the gas flow of ≈ 96.5°C temperature, the water droplets equilibrium evaporation temperature is ≈ 42.5°C, when the volumetric fraction of water vapour is 0.0129 in the air. After the additionally humidifying the air flow up to $\bar{p}_v = 0.045$, the water droplets equilibrium evaporation temperature increases to ≈ 55°C. When the gas flow of ≈ 85.6°C temperature and the volumetric fraction of water vapour is 0.0087 the droplets equilibrium evaporation temperature is ≈ 33.5°C. In the additionally humidified gas flow of ≈ 81°C temperature, the water droplets equilibrium evaporation temperature rises to a higher ≈ 58.5°C in transient phase change regime, when the volumetric fraction of water vapour is 0.144 in the gas.
4. The instantaneous boundary conditions of the heat transfer also have a certain influence on the thermal state of the droplet equilibrium evaporation. Owing to the different equivalent droplet diameter at the beginning of the equilibrium evaporation, the heterogeneity of a droplet is determined by the uneven convective heating, although the air flow parameters are similar. This explains

the inconsistency between the measured equilibrium evaporation temperatures of ≈ 1.5°C and ≈ 3°C when the air flow parameters are similar in the first and second parts of experiments.

5. Water injection must be organized for individual units of biofuel combustion technologies in a targeted and coordinated manner. Only then will it be possible to achieve the optimal process of heat recovery from the biofuel flue gas and ensure a high efficiency in biofuel combustion technology. Because the volumetric fraction of water vapour can range from 0.2 to 0.4 in a humid biofuel flue gas, the temperature of the equilibrium evaporation of the injected water droplets can be significantly higher, and sequentially decrease during the flue gas drying process. For a more detailed assessment, a broader experiment is needed.

References

1. **Kriegler, E.;** et. all. 2017. Fossil-fuelled development: An energy and resource intensive scenario for the 21st century, Global Environmental Change 42: 297-315. https://doi.org/10.1016/j.gloenvcha.2016.05.015.
2. **Wood, N.; Roelich, K.** 2019. Tensions, capabilities, and justice in climate change mitigation of fossil fuels, Energy Research and Social Science 52: 114-122. https://doi.org/10.1016/j.erss.2019.02.014.
3. **Handayani, K; Krozer, Y; Filatova, T.** 2019. From fossil fuels to renewables: an analysis of long-term scenarios considering technological learning, Energy Policy 127: 134-136. https://doi.org/10.1016/j.enpol.2018.11.045.
4. **Borawski, P.;** et. all. 2019. Development of renewable energy sources market and biofuels in The European Union, Journal of Cleaner Production 228: 467-484. https://doi.org/10.1016/j.jclepro.2019.04.242.
5. **Agugliaro, M. F.; Alcayde, A.; Montoya, F.; Zapata-Sierra, A.; Gil, C.** Scientific production of renewable energies worldwide: An overview, Renewable and Sustainable Energy Reviews 18: 134-143. https://doi.org/10.1016/j.rser.2012.10.020.
6. **Dunn, J. B.** 2019. Biofuel and bio product environmental sustainability analysis, Current Opinion in Biotechnology 57: 88-93. https://doi.org/10.1016/j.copbio.2019.02.008.
7. **Tudo, J. L. A.; Cogollos, L. C.; Aleixandre, J. L.; Benavent, R. A.** 2019. Renewable energies: Worldwide trends in research, funding and international collaboration, Renewable Energy 139: 268-278. https://doi.org/10.1016/j.renene.2019.02.079.
8. **Trojanowski, R.; Fthenakis, V.** 2019. Nanoparticle emissions from residential wood combustion: A critical literature review, characterization, and recommendations, Renewable and Sustainable Energy Reviews 103: 515-528. https://doi.org/10.1016/j.rser.2019.01.007.
9. **Agarwal, A. K.** 2007. Biofuels (alcohols and biodiesel) applications as fuels for internal combustion engines, Prog. in Energy and Combustion Science 33: 233-271. https://doi.org/10.1016/j.pecs.2006.08.003.
10. **Arifin, Y.; Tanudjaja, E.; Dimyati, A.; Pinontoan, R.** 2014. A second generation biofuel from cellulosic agricultural by-product fermentation using species for electricity generation, Energy Procedia 47: 310-315. https://doi.org/10.1016/j.egypro.2014.01.230.
11. **Kruczek, H. P.; Ostrycharczyk, M.; Zgora, J.** 2013. Co-combustion of liquid biofuels in PC boilers of 200 MW utility unit, Proceedings of the Combustion Institute 34: 2769-2777. https://doi.org/10.1016/j.proci.2012.08.010.
12. **Lavric, L. D.; Konnov, A. A.; Ruyckf, J. D.** 2004. Dioxin levels in wood combustion—a review, Biomass and Bioenergy 26: 115-145. https://doi.org/10.1016/S0961-9534(03)00104-1.
13. **Drabik, D.; Venus, T. J.** 2017. Water Use for Biofuels in Europe, Competition for Water Resources / Experiences and Management Apr. in the US and Europe: 144-159. https://doi.org/10.1016/B978-0-12-803237-4.00008-2.
14. **Farooq, W.; Suh, W. I.; Park, M. P.; Yang, J. W.** 2015. Water use and its recycling in microalgae cultivation for biofuel application, Bioresource Technology 184: 73-81. https://doi.org/10.1016/j.biortech.2014.10.140.
15. **Dechambre, D.; Thien, J.; Bardow, A.** 2017. When 2nd generation biofuel meets water – The water solubility and phase stability issue, Fuel 209: 615-623. https://doi.org/10.1016/j.fuel.2017.07.110.
16. **Dogaris, I.; Loya, B.; Cox, J.; Philippidis, G.** 2019. Study of landfill leachate as a sustainable source of water and nutrients for algal biofuels and bioproducts using the microalga Picochlorum oculatum in a novel scalable bioreactor, Bioresource Technology 282: 18-27. https://doi.org/10.1016/j.biortech.2019.03.003.
17. **Yang, B.; Chen, H.** 2019. Heat and water recovery from flue gas: Application of micro-porous ceramic membrane tube bundles in gas-fired power plant, Engineering a Chemical and Processing - Process Intensification 137: 116-127. https://doi.org/10.1016/j.applthermaleng.2016.08.191.
18. **Yang, S.; Han, Z.; Pan, X.; Liu, B,; Zhao, D.** 2018. Nitrogen oxide removal from simulated flue gas by UV-irradiated electrolyzed seawater: Efficiency optimization and pH-dependent mechanisms, Chemical Engineering Journal 354: 653-662. https://doi.org/10.1016/j.cej.2018.07.191.
19. **Barata, J.** 2008. Modelling of biofuel droplets dispersion and evaporation, Ren. Energy 33: 769-779. https://doi.org/10.1016/j.renene.2007.04.019.
20. **Arpornpong, N.; Attaphong, C.; Charoensaeng, A.; Sabatini, D. A.; Khaodhiar, S.** 2014. Ethanol-in-palm oil/diesel microemulsion-based biofuel: Phase behavior, viscosity, and droplet size, Fuel 132: 101-106. https://doi.org/10.1016/j.fuel.2014.04.068.
21. **Liu, Y. C.; Savas, A. J.; Avedisian, C. T.** 2013. The spherically symmetric droplet burning characteristics of Jet-A and biofuels derived from camelina and tallow, Fuel: 824-832. https://doi.org/10.1016/j.fuel.2014.04.068.
22. **Morin, C.; Chauveau, C.; Gokalp, I.** 2000. Droplet vaporization characteristics of vegetable oil derived biofuels at high temperatures, Experimental Thermal and Fluid Science 21: 491-502. https://doi.org/10.1016/S0894-1777(99)00052-7.
23. **Cordoba, P.;** et. al. 2011. Enrichment of inorganic trace pollutants in recirculated water streams from a wet limestone flue gas desulphurisation system in two coal power plants, Fuel Proces. Technology 92: 1764-1775. https://doi.org/10.1016/j.fuproc.2011.04.025.

24. **Namioka, C. T.; Yoshikawa, K.; Takeshita, M.; Fujiwara, K.** 2012. Commercial-scale demonstration of pollutant emission reduction and energy saving for industrial boilers by employing water/oil emulsified fuel, Applied Energy 93: 517-522. https://doi.org/10.1016/j.apenergy.2011.12.018.
25. **Calinescu, I.; Martin, D.; Chmielewski, A.; Ighigeanu, D.** 2013. E-Beam SO_2 and NO_x removal from flue gases in the presence of fine water droplets, Radiation Physics and Chemistry 85: 130-138. https://doi.org/10.1016/j.radphyschem.2012.10.008.
26. **Voytkov, I.; Volkov, R.; Strizhak, P.** 2017. Reducing the flue gases temperature by individual droplets, aerosol, and large water batches, Experimental Thermal and Fluid Science 88: 301-316. https://doi.org/10.1016/j.expthermflusci.2017.06.009.
27. **Miliauskas, G.; Maziukienė, M.; Jouhara, H.; Poškas, R.** 2019. Investigation of mass and heat transfer processes of water droplets in wet gas flow in the framework of energy recovery technologies for biofuel combustion and flue gas removal, Energy 173: 740-754. https://doi.org/10.1016/j.energy.2019.02.101.
28. **Paepe, H. W.; Carrero, M.; Bram, S.; Contino, F.; Parente, A. Q.** 2017. Waste heat recovery optimization in micro gas turbine applications using advanced humidified gas turbine cycle concepts, Applied Energy 207: 218-229. https://doi.org/10.1016/j.apenergy.2017.06.001.
29. **Fuchs, N. A.** 1959. Evaporation and droplet growth in gaseous media. London: Pergamon Press: 41. https://doi.org/10.1016/B978-1-4832-0060-6.50002-8.
30. **Shazin, S. S.** 2014. Droplets and Sprays, Springer, Heidelberg: 342. https://doi.org/10.1007/978-1-4471-6386-2.
31. **Breitenbach, J.; Rosiman, V. I.; Tropea, C.** 2017. Heat transfer in the film boiling regime: Single drop impact and spray cooling, International Journal of Heat and Mass Transfer 110: 34-42. https://doi.org/10.1016/j.ijheatmasstransfer.2017.03.004.
32. **Mingrui, W.; Nguyen, T. S.; Turkson, R. F.; Jinping, J.; Guanlun, G.** 2017. Water injection for higher engine performance and lower emissions, Journal of Energy Institute 90: 285-299. https://doi.org/10.1016/j.joei.2015.12.003.
33. **Sirignano, W. A.** 2000. Fluid Dynamics and Transport of Droplets and Sprays, Cambridge University Press: 311. https://doi.org/10.1017/CBO9780511529566.
34. **Miliauskas, G.; Maziukiene, M.; Ramanauskas, V.; Puida, E.** 2017. The defining factors of the phase change cycle of water droplets that are warming in humid gas, International Journal of Heat and Mass Transfer 113: 683-703. https://doi.org/10.1016/j.ijheatmasstransfer2017.05.129.
35. **Tseng, C. C.; Viskanta, R.** 2006. Enhancement of water droplet evaporation by radiation absorption, Fire Safety Journal 41: 236-247. https://doi.org/10.1016/j.firesaf.2006.01.001.
36. **Brewster, M. Q.** 2015. Evaporation and condensation of water mist/cloud droplets with thermal radiation, International J. of Heat and Mass Transfer 88: 236-247. https://doi.org/10.1016/j.ijheatmasstransfer.2015.03.055.
37. **Marques, O.** 2011. Practical Image and Video Processing Using MATLAB. Wiley-IEEE Press: 451. https://doi.org/10.1002/9781118093467.
38. **Vukalovitch, M. P.** 1958. Thermodynamics properties of water and steam, VEB Verlag Technik, Berlin: 245.
39. **Abramzon, B.; Sirignano, W. A.** 1989. Droplet vaporization model for spray combustion calculations, International Journal of Heat and Mass Transfer 32: 1605–1618. https://doi.org/10.1016/0017-9310(89)90043-4.

V. Ramanauskas, E. Puida, G. Miliauskas, L. Paukštaitis

EXPERIMENTAL INVESTIGATION OF WATER DROPLET HEATING IN HUMIDIFIED AIR FLOW

S u m m a r y

An experimental research method and an analysis of the results of a water droplet heating in the additionally humidified air flow are presented. The variation of the thermal state of convectively heated water droplets are determined. In the gas flow the factors determining the phase change regimes of a water droplets are the humidity of the air and the initial temperature of the water. The influence of initial water temperature on the thermal state of a droplet in transient phase change regime is experimentally substantiated.

Keywords: additionally humidified air, water droplet heating, experimental investigation.

Received July 09, 2019
Accepted November 21, 2019